

Visual intensity ratio modulates operant learning responses in larval zebrafish

1 **Wenbin Yang^{1,2*}, Yutong Meng^{1,2}, Danyang Li^{1,2}, Quan Wen^{1,2,3*}**

2 ¹Center for Integrative Imaging, Hefei National Laboratory for Physical Sciences at
3 Microscale, School of Life Sciences, University of Science and Technology of China,
4 Hefei, China

5 ²Chinese Academy of Sciences Key Laboratory of Brain Function and Disease, Hefei,
6 China

7 ³Center for Excellence in Brain Science and Intelligence Technology, Chinese
8 Academy of Sciences, Shanghai 200031, China

9 *** Correspondence:**

10 young24@mail.ustc.edu.cn, qwen@ustc.edu.cn

11 **Keywords: zebrafish larvae, behavioral neuroscience, learning, vision,**
12 **high-throughput imaging, automated image analysis**

13 **Abstract**

14 Larval zebrafish is a promising vertebrate model for understanding neural
15 mechanisms underlying learning and memory. Here, we report on a high-throughput
16 operant learning system for zebrafish larvae and demonstrate that lower visual
17 intensity ratio of the conditioned stimulus to the background can enhance learning
18 ability, highlighted by several behavioral metrics. We further characterize the learning
19 curves as well as memory extinction for each conditioned pattern. Finally, we show
20 how this learning process developed from 7 days old to 10 days old zebrafish.

21 **Highlights**

- 22 • Conditioned visual patterns with lower intensity ratio to the background elicited
- 23 stronger operant learning responses
- 24 • Memory extinction was modulated by the visual intensity ratio of the conditioned
- 25 stimulus to the background
- 26 • A high-throughput automated system for acquiring and analyzing behavioral data

27

28 **1 Introduction**

29 In operant conditioning, an animal learns, through trial and error, to correlate its
30 behavioral responses with the consequences. This form of associative learning has
31 been intensively studied in mammals (Freund and Walker, 1972; Ishikawa et al.,
32 2014), but the biological learning rules, as well as their implementation by the brain
33 circuit, remains elusive. To make progress, it would be illuminating to measure neural
34 activities of defined cell types at the whole-brain scale during the entire learning
35 process. Larval zebrafish is a promising vertebrate model for this purpose: the
36 transparency and the relatively small brain is a great compromise between system
37 complexity and simplicity. Recently, it has become possible to perform the
38 whole-brain imaging of calcium activities in freely behaving larval zebrafish (Cong et
39 al., 2017; Kim et al., 2017). Whereas fish are well-established animal models to study
40 learning and memory (Agranoff and Davis, 1968; Davis and Agranoff, 1966), few
41 associative learning paradigms have been developed for zebrafish larvae. Li (Li, 2012)
42 reported operant learning in head-fixed larvae with aversive heat stimulus; Valente
43 and colleagues (Valente et al., 2012) showed that one-week larvae were unable to
44 perform an operant learning paradigm, in which fish must learn to swim to the other
45 half of an arena to avoid electroshocks. Other reports demonstrated that larval
46 zebrafish could also learn classical conditioning: they could associate the conditioned
47 stimulus (CS), a moving spot, with the unconditioned stimulus (US), a touch of the
48 body (Aizenberg and Schuman, 2011). Social reward, such as visual access to
49 conspecifics, could also be paired with a distinct visual environment during classical
50 conditioning in larval zebrafish (Hinz et al., 2013).

51 Zebrafish have sophisticated vision: they can discriminate size, color, intensity and
52 object motion with ease. Spatial and non-spatial visual learning tasks have been well
53 studied in adult zebrafish (Arthur and Levin, 2001). However, much less is known
54 about how visual properties would modulate the learning process in larval zebrafish.
55 Here, we reported a modified operant conditioning paradigm (Valente et al., 2012) in
56 freely swimming larval zebrafish, a system that combines a high-throughput
57 automated training process and a toolkit for post-data analysis and storage. We used
58 our new paradigm to investigate how visual intensity ratio modulated the operant
59 learning responses in larvae, characterized by both positional and turning metrics. We
60 also quantified the learning curves and memory extinction for individuals.

61 **2 Material and Methods**

62 **2.1 Ethical statement of animals-using**

63 Handling and care of all animals were conducted in strict accordance with the
64 guidelines and regulations set forth by University of Science and Technology of
65 China (USTC) Animal Resources Center, and University Animal Care and Use
66 Committee. Both raising and training protocols were approved by the Committee on
67 the Ethics of Animal Experiments of the USTC (permit number:
68 USTCACUC1103013).

69 **2.2 Animals and raising**

70 Zebrafish (*Danio rerio*) of the genotype huc:h2b-gcamp6f were used in all
71 experiments. All tested fish were from 7 to 10 dpf (day past fertilization) larvae. They
72 were bred, raised and housed in the same environment. Fish were fed two times per
73 day from 6 dpf with paramecium in the morning (8-9 A.M.) and evening (6-7 P.M.)
74 until used in the experiments. Water was replaced with E2 medium (Cunliffe, 2003)
75 in the morning (8-9 A.M.) and evening (6-7 P.M.). Water temperature was maintained
76 at 28.5 °C. Illumination was provided by fluorescent light tubes from the ceiling with
77 lights turned on at 08:00 A.M. and off at 10:00 P.M.

78 **2.3 Experimental Setup**

79 The behavioral system with custom software suites and supported hardware were built
80 to achieve an end-to-end high-throughput experimental workflow. (Figure 1A)

81 **2.3.1 Hardware**

82 Zebrafish swam freely in custom-built acrylic containers with transparent bottoms.
83 Each container was divided into four arenas separated by opaque walls. The arena's
84 size is 3 cm × 3 cm × 1 cm, with water filled (Fig. S2.a). Each arena held one fish.
85 Three CMOS cameras (Basler aca2000-165umNIR, Germany) with adjustable lens
86 (Canon, Model EF-S 18-55mm f/3.5-5.6 IS II, Japan) simultaneously captured
87 swimming behavior at ten frames per second. Three infrared LED light sources
88 (Kemai Vision, China, model HF-FX90, wavelength 940 nm) illuminated each
89 container from below. A 700 nm long-pass filter (Thorlabs FEL0700, US.) was
90 positioned in front of each camera to block visible light to facilitate online imaging
91 processing with custom software BLITZ. Visual stimuli were presented by a projector
92 from the top over all three containers (PIQS Projector S1, 14.6 × 7.85 × 1.75 cm, 854
93 × 480 pixels). Electroshocks (100 ms, 9 Volt/3 cm) were delivered via two platinum
94 filaments, one on each side of the arena. Shock delivery at each arena was controlled
95 by custom software BLITZ via a 16-channels relay (HongFa JQC-3FF, China). Room
96 temperature was controlled by an air-conditioner at 27 °C.

97 **2.3.2 Software Suites**

98 Custom C++ software BLITZ (Behavioral Learning In The Zebrafish, inheriting the
99 coding style from MindControl (Leifer et al., 2011)) with Microsoft Visual Studio
100 2017 processed three video streams in parallel to get real-time head, center, tail
101 positions and heading angle by using the Pylon library (Basler AG, Germany) and the
102 open source computer vision library (OpenCV) (Bradski, 2000). The program also
103 rendered visual pattern and programmable electroshocks delivery based on the
104 timeline and real-time fish motion parameters. All necessary experimental
105 information (e.g., experiment start time, visual pattern index, shocks delivery
106 information, and fish motion parameters) were recorded in YAML files. Raw videos
107 were recorded.

108 The BLITZ software is available at <https://github.com/Wenlab/BLITZ>.

109 Another custom MATLAB (The MathWorks, Inc.) software ABLITZER (the
110 Analyzer of BLITZ Results) was used to import YAML files, to visualize data, as
111 well as to perform the behavioral and statistical analysis.

112 The ABLITZER software is available at <https://github.com/Wenlab/ABLITZER>.

113 **2.4 Experimental Procedure**

114 Fish were fed at least an hour before using in the experiment. Fish were placed via a
115 Pasteur pipette (Nest, US) from the raising tank to the experimental arenas. The
116 behavioral experiment would not run until fish started moving around to avoid startle
117 responses to novel stimuli. Fish in the paired-group were trained first with the
118 self-control protocol (see below), then with the operant learning protocol. Fish in the
119 unpaired-group were trained first with the self-control protocol, then with the
120 unpaired operant learning protocol (see below).

121 Fish used in the paired-group and unpaired-group were all naive fish before the
122 experiment.

123 **2.4.1 Operant learning protocol**

124 This operant learning protocol was modified from Valente's learning paradigm
125 (Valente et al., 2012). Here, fish would experience four different phases in order:
126 baseline phase, training phase, blackout phase and test phase. (Figure 2B)

127 First, in the 10 minutes baseline phase, the visual pattern beneath each arena would
128 flip between the CS at the top (Figure S1A, C or E) and the CS at the bottom (Figure
129 S1B, D or F) with a random duration that was uniformly sampled from 30 to 45
130 seconds.

131 Second, in the 20 minutes training phase, both the update of visual patterns and the
132 delivery of electroshocks were dependent upon fish's behavior. After the visual
133 pattern was updated (including the first visual pattern in the training stage), fish had 7
134 seconds thinking-time to escape from the CS zone. If fish were in the CS zone after
135 the thinking time, whole-arena shocks would be delivered every 3 seconds until fish
136 escaped from the CS zone. After fish stayed in the Non-CS zone for 48 seconds, the
137 visual patterns (CS zone at the top or bottom) would update with equal probability.
138 The whole procedure would repeat (Figure 1B).

139 After the training phase, there was a one-minute blackout phase to deprive all visual
140 stimuli.

141 Finally, in the last 18 minutes test phase, to ask whether fish could develop the
142 association between the CS pattern and the US shock, the visual pattern interchanges
143 every two minutes between at the top and at the bottom until the end.

144 **2.4.2 Self-control conditioning protocol**

145 All phases were identical to the operant learning protocol, except for no electroshock
146 delivery.

147 **2.4.3 Unpaired operant learning protocol**

148 All phases were identical to the operant learning protocol except for the training phase,
149 in which electroshocks, without pairing with visual patterns, were randomly delivered
150 across the 20-minute duration.

151 **2.5 Behavioral Analysis**

152 **2.5.1 Visual intensity ratio**

153 The visual intensity ratio is defined as the ratio of the grayscale value of the
154 conditioned pattern to the grayscale value of the pure-gray pattern (the
155 non-conditioned pattern). The descending ranking of intensity ratios: the white-black
156 checkerboard > the red-black checkerboard > the pure-black pattern (see Table. 1 for
157 more details).

158 **2.5.2 Pre-screening**

159 We define data quality as the percentage of not-bad frames. Frames when fish froze
160 over 1 second were considered bad. Fish with data quality lower than 0.95 were
161 excluded from the analysis since those fish did not swim spontaneously and
162 frequently. Those fish were considered not in good conditions.

163 The positional index is defined as the percentage of frames when fish were in the
164 non-CS zone.

165 **2.5.3 Turning analysis**

166 We scored a turning event when the heading angle change between two consecutive
167 frames exceeded 15 degrees. The fish would get +1 score when performing an escape
168 turn, and -1 score when returning to the CS zone. Fish in the Non-CS zone executed
169 an escape turn when they approached the midline (within twice body length) and then
170 turned back (Figure S2). The turning index is defined as

$$171 \quad \text{turning index} = \frac{1}{2} + \frac{s(+)+s(-)}{(|s(+)|+|s(-)|)\cdot 2}$$

172 where $s(+)$ and $s(-)$ are positive and negative scores respectively. In this way, the
173 turning index would fall between 0 and 1, the same range as the positional index.

174

175 **2.5.4 Distance to the mid-line**

176 This is defined as a signed Euclidean distance from the fish head position to the
177 mid-line. The sign is -1 when fish were in the CS zone and +1 when fish were in the
178 non-CS zone.

179 **2.5.5 Learning analysis**

180 To evaluate whether fish learned the operant learning task, we divided the entire
181 operant conditioning protocol time into 24 two-minute-epochs. The memory may go
182 extinct during the test phase in the absence of electroshocks (Myers and Davis, 2007).
183 The extinction point was computed as the first time when the positional index within
184 an epoch dropped below the baseline. The retrievable period was defined from the
185 starting time of the test phase to the extinction point. We would use the memory
186 length or the retrievable period interchangeably. If the positional indices in the
187 retrievable period were significantly higher than the positional indices in the baseline
188 phase, fish were classified as learners (The unpaired t-test was applied).

189 The positional index increment is the difference between the mean positional index in
190 the retrieval period and the mean index in the baseline period. And the turning index
191 increment is the difference between the mean turning index in the retrieval period and
192 the mean index in the baseline period. The learning ratio is the ratio of the number of
193 learners to the total number of fish.

194 **2.6 Statistical Analysis**

195 The paired t-tests were used to compare the difference between fish trained with the
196 self-control conditioning protocol and the operant conditioning protocol; whereas the
197 unpaired t-tests were used for the comparison between fish trained with the unpaired
198 operant control protocol and those with operant learning protocol. The sample size
199 exceeded 20 for all tests.

200 **2.7 Linear Regression**

201 The linear regression model

$$202 \quad y = \beta_0 + \beta_1 x,$$

203 where β_0 , β_1 were linear coefficients, was used to statistically quantify the trend of
204 learning versus ages in terms of memory length, positional index increment, and
205 turning index increment. Estimated linear coefficients, R-squared coefficients, and
206 p-values for F-tests on the model were calculated using fitlm in the MATLAB
207 Statistics and Machine Learning Toolbox.

208

209 **3 Results**

210 **3.1 Larval zebrafish show significant learning responses in the operant** 211 **learning task**

212 **3.1.1 A high-throughput behavioral system for the operant learning task**

213 In our modified operant learning task (Figure 1B), larval zebrafish freely swam in an
214 arena divided by two distinct patterns, each of which was projected onto one half of a
215 transparent floor. In all cases, a pure-gray visual pattern was presented in the non-CS
216 zone, whereas other patterns were presented on the other half as the CS. The CS was
217 paired with the US, moderate electroshocks. The delivery of the US and the update of
218 visual patterns depended upon fish's positions (see Material and Methods for detailed
219 experimental procedures).

220 To scale up the learning process, we developed a high-throughput operant
221 conditioning system (Figure 1A) with supporting software suites BLITZ and
222 ABLITZER (see Material and Methods) that allowed training 12 fish simultaneously.
223 BLITZ provided a fully automated workflow from video capture, online image
224 processing, to visual stimulus presentation and electroshocks delivery for all
225 behavioral protocols. Raw experimental data were then imported, analyzed and
226 visualized by ABLITZER.

227 **3.1.2 Larval zebrafish show significant learning responses in the operant** 228 **learning task**

229 We found that 7-10 dpf zebrafish larvae showed significant learning responses
230 (Figure 1C and Figure 1D), evaluated based on fish positions — positional index and
231 turning index (see Material and Methods). Because larval zebrafish have the innate
232 positive light preference, we developed two control settings: a self-control
233 conditioning protocol in which no electroshock were delivered and an unpaired
234 operant learning protocol in which electroshocks were randomly delivered (see
235 Material and Methods). Results from the two control settings were compared with
236 those from operant learning protocol to determine whether fish learned the association.
237 Figure 1E shows a representative trajectory of a learner who tended to avoid
238 conditioned visual pattern after training.

239 **3.2 Visual intensity ratio modulates operant learning responses in larval** 240 **zebrafish**

241 We asked whether visual intensity ratios — CS patterns with different mean
242 intensities to the non-CS pattern (pure-gray pattern) — would modulate learning.
243 Indeed, the lower CS to non-CS intensity ratio led to stronger learning responses: the
244 group of fish presented with the white-black checkerboard showed almost no learning
245 response (Figure 2A and Figure 2B), whereas those presented with the pure-black
246 pattern showed prominent learning responses (Figure 2C and Figure 2D), quantified

247 by the positional index and turning index. The learning indices for fish presented with
248 the red-black checkerboard fell in between the two other cases (Table 2).

249 **3.3 Single fish analysis distinguishes learners from non-learners**

250 After the population analysis of learning responses, we next focused on individuals,
251 e.g., to count learners. Here, we divided the entire process into epochs. Every
252 two-minute-interval was one epoch. Therefore, the baseline phase has five epochs; the
253 training phase has ten epochs, and the test phase has nine epochs.

254 **3.3.1 Memory extinction**

255 We define the memory extinction point as the first time when the positional index
256 within an epoch drops below the index in the baseline phase, and define the duration
257 from the start of the test phase to the extinction point as the memory length. Memory
258 length shorter than two epochs (e.g., fish may stay still in the non-CS zone) were
259 excluded (see Material and Methods).

260 **3.3.2 Single fish analysis**

261 Fish were categorized as learners only when their positional indices across the
262 memory length were significantly higher than the indices in the baseline phase (see
263 Material and Methods). We found that 26% of the fish were learners when the CS was
264 red-black checkerboard (N = 104), and 50% of the fish were learners when the CS
265 was pure-black pattern (N = 42). When white-black checkerboard was used as the CS,
266 only one out of 37 fish learned (Table 3). The learners' group showed significant
267 changes in both the mean positional index and turning index before and after training
268 (Figure 3B, C and Figure 3E, F).

269 We plotted the learning curve — positional indices versus time — for learners and
270 non-learners (Figure 3A). In the case of red-black checkerboard learners, the learning
271 curve rose and approached the maximum near the end of training; during the test
272 phase, the learning curve remained high during the first three epochs before memory
273 extinction. In Figure 3G, we showed the trace of a typical fish with memory
274 extinction in the test phase. Figure 3H magnified the test phase of Figure 3G, in which
275 after the extinction point at ~ 37 minute, fish started to swim more in the CS-zone.

276 In the case of pure black pattern learners, the learning curve also reached its
277 maximum near the end of training. However, it remained high across the entire test
278 phase (Figure 3D).

279 In Figure 3I, we compared the distribution of memory lengths when two different CS
280 patterns were used. The mean memory length in the red-black checkerboard case was
281 756 seconds whereas the mean memory length lasted 970 seconds in the pure-black
282 pattern case. Also, all black pattern learners' memory lengths were longer than 480
283 seconds.

284

285 **3.4 Age-dependent operant learning in larval zebrafish**

286 We evaluated the learning abilities across 7-10 dpf larval zebrafish by plotting the
287 memory length, positional index and turning index versus ages.

288 In the case of learning red-black checkerboard pattern, the positional index increment
289 (see Material and Methods) and the memory length shows an increasing trend from 7
290 dpf to 10 dpf (Figure 4A and Figure 4B). However, there is no such trend in the
291 turning index increment (see Material and Methods and Figure 4C).

292 In the case of learning the black visual pattern, however, no increasing trends from 7
293 dpf to 10 dpf fish were found for the memory length (Figure 4D), the positional index
294 increment (Figure 4E) and the turning index increment (Figure 4F).

295 **4 Discussion**

296 **4.1 Operant learning in larval zebrafish**

297 Operant learning allows animals to avoid dangers or to find potential rewards in a
298 complex environment (Skinner, 1984). In this study, we demonstrated 7-10 dpf larval
299 zebrafish showed significant operant learning responses when the CS, for example a
300 red-black checkerboard pattern, was paired with the US, noxious electroshocks. In an
301 earlier study (Valente et al., 2012), it was reported that one-week larvae showed no
302 significant learning response. Several factors may explain this discrepancy. First, we
303 observed little learning response when the white-black checkerboard was paired with
304 the US (only one fish learned the contingency), consistent with Valente's results.
305 Enhancement of learning was observed, however, when the red-black checkerboard
306 was paired with the US. In both cases, the non-CS zone was pure gray. The red-black
307 checkerboard has a lower visual intensity ratio than the white-black checkerboard (see
308 Table 1), and we hypothesize that visual intensity could strongly modulate the
309 learning response. Second, in our modified paradigm, fish had more opportunity to
310 learn the contingency between the CS and the US during the training period: when
311 fish stayed in the non-CS zone for more than 48 seconds, the positions of the CS and
312 non-CS patterns would update. In Valente's paradigm, however, there were no visual
313 pattern updates when fish stayed within the non-CS zone.

314 **4.2 Visual intensity ratio modulates learning in larval zebrafish**

315 We further investigated whether different visual intensity ratios could modulate
316 learning ability in larval zebrafish. We found that fish showed little learning response
317 when the white-black checkerboard was used as the CS pattern, which has the same
318 average intensity as pure gray, the non-CS visual pattern. However, when the
319 red-black checkerboard or pure-black visual pattern was used, some fish (28% in the
320 group exposed to the red-black checkerboard and 50% exposed to the pure-black
321 pattern) showed strong learning responses. Moreover, both the positional index and
322 turning index were significantly higher in fish exposed to pure-black visual pattern
323 versus those exposed to the red-black checkerboard (see Table 2).

324 Many studies have demonstrated that larval zebrafish exhibit positive phototaxis
325 (Steenbergen et al.2011; Chen and Engert 2014; Guggiana-Nilo and Engert 2016). In
326 our behavioral paradigm, the behavioral metric baselines (e.g., positional index) were
327 computed first from a self-control procedure (see Material and Methods) before the
328 operant learning procedure started. Visual intensity ratio could shift the baselines (see
329 Table 2) due to animal's innate bias. Significant changes of the behavioral metrics
330 during and after operant learning (see Figure 2), however, require an explanation that
331 goes beyond innate avoidance responses.

332 Here we speculate that intensity-ratio-dependent learning may arise from the crosstalk
333 between the phototaxis and fear learning circuits. Both the phototaxis and
334 US-triggered fear responses involve habenula (Agetsuma et al., 2010; Zhang et al.,
335 2017), a specialized brain region where a direct association of the CS with fear may
336 occur through synaptic plasticity. According to this model, the CS would trigger fear
337 responses, and learning leads to a stronger association of the visual-related input and
338 the escape response. These predictions can potentially be tested by combining our
339 behavioral system with whole brain calcium imaging in freely behaving larval
340 zebrafish (Cong et al., 2017).

341 **4.3 Memory extinction**

342 Memory extinction is an active learning process where an animal learns to dissociate
343 the conditioned response and the CS in the absence of the US (Myers and Davis,
344 2007). In our assay, the extinction point is defined as the first epoch whose positional
345 index dropped below the mean positional index of the baseline. In addition, fish that
346 did not keep a high level of the positional index for at least two epochs were not
347 counted (see Material and Methods). When the red-black checkerboard was used as
348 the CS, memory lengths were distributed within a range of 7-18 minutes (Figure 3I),
349 consistent with a recent classical conditioning paradigm in larval zebrafish (Aizenberg
350 and Schuman, 2011). When the pure-black pattern was used as the CS, few learners
351 showed memory extinction before the 18-minute test phase ended (see Figure 3G).
352 Taken together, these results suggest that both operant conditioning and memory
353 extinction could be differentially modulated by the visual intensity ratio.

354 **4.4 Development of Operant Learning in Larvae**

355 We selected 7-10 dpf zebrafish larvae for operant conditioning, a choice that was
356 based on two considerations. First, larvae at 6 dpf show frequent long-pauses (over 7
357 seconds), and therefore are not suitable for operant conditioning: an animal must
358 explore the action space instead of staying still. Second, an earlier work (Ingebretson
359 and Masino, 2013) found that larvae at 7 dpf and later will produce more consistent
360 locomotor activities. Here we found that 10 dpf fish exhibited the longest memory
361 length when the red-black checkerboard was used as the CS; whereas 7 dpf fish
362 showed the shortest memory length when the pure-black pattern was used (see Figure
363 4A). In addition, in the case of associating the red-black checkerboard pattern with the
364 US, there is an age-dependent increasing trend for the memory length (Figure 4A) and

365 the positional index increment (Figure 4B). No such trends were found when the
366 pure-black pattern was used as CS (see Figure 4D, E, and F). These differences may
367 partially result from a continuous development of larval zebrafish brain (Mueller and
368 Wullimann, 2013).

369 **4.5 High-throughput behavioral assays for learning and memory in Larval** 370 **Zebrafish**

371 Larval zebrafish are amenable to high-throughput screen due to their transparency,
372 small size and high permeability to small molecules (Kokel et al., 2010; Rihel et al.,
373 2010). Though most high-throughput systems are designed for drug or genetic screens
374 (Gehrig et al., 2018; Rihel et al., 2010; Yang et al., 2018), here we have developed a
375 high-throughput behavioral training system with custom supported software suites.
376 Compared with previous work (Hinz et al., 2013; Pelkowski et al., 2011), the BLITZ
377 software has enabled a fully automatic control of video capture, online image
378 processing, visual pattern presentation and electroshocks delivery, making it an easily
379 adaptable system for various purposes. Our complementary ABLITZER software also
380 allows users to import, analyze and visualize data with well-structured classes and
381 functions.

382 So far, our system cannot deal with situations of overlapping larvae, whose identities
383 are hard to assign based on the current tracking algorithm. An earlier work (Mirat et
384 al., 2013) showed that accurately tracking multiple larvae in groups over long periods
385 of time were feasible. Integration of their algorithm with BLITZ may allow the study
386 of social interactions of larval zebrafish in the future (Buske and Gerlai, 2014).

387 In conclusion, we have developed a high-throughput operant conditioning system for
388 larval zebrafish. When using electroshocks as the US and red-black checkerboard or
389 pure-black pattern as the CS, we demonstrated that a fraction of larval zebrafish could
390 acquire operant learning, and the performances strongly depended on the visual
391 intensity ratio of the CS to the non-CS pattern. Finally, we also identified
392 age-dependent learning variability across 7-10 dpf larval zebrafish.

393 **5 Conflict of interest**

394 The authors declare that the research was conducted in the absence of any commercial
395 or financial relationships that could be construed as a potential conflict of interest.

396 **6 Author Contributions**

397 Wenbin Yang conceived the study, designed and built the behavioral setup, developed
398 the software suites, designed, carried out the experiments, wrote the manuscript and
399 conceived the figures.

400 Yutong Meng helped carry out the experiment and conceive the figures.

401 Danyang Li helped design, build the behavioral setup and conceive the figures.

402 Quan Wen helped design the experiments and wrote the manuscript.

403 **7 Funding**

404 This work was funded by National Science Foundation of China Grants NSFC-
405 31471051 and NSFC-91632102, the Strategic Priority Research Program of the
406 Chinese Academy of Sciences (Pilot study, grant XDPB10).

407 **8 Acknowledgments**

408 The authors would like to thank Bing Hu for kindly providing the housing for
409 zebrafish, Yuming Chai, Kexin Qi and Kun He for invaluable technical help; Florian
410 Engert, Caroline Wee, Max Nikitchinko and Armin Bahl for kind guidance and
411 inspirations in behavioral neuroscience.

412 **9 Supplementary Material**

413 The Supplementary Material for this article can be found in the attachment.

414 **10 Abbreviations**

415 dpf, days post fertilization; fps, frames per second; SEM, standard error of the mean;
416 BLITZ, behavioral learning in the zebrafish; ABLITZER, the analyzer of BLITZ
417 results

418 **11 Data Availability Statement**

419 Datasets are available on request.

420 **12 References**

- 421 Agetsuma, M., Aizawa, H., Aoki, T., Nakayama, R., Takahoko, M., Goto, M., et al.
422 (2010). The habenula is crucial for experience-dependent modification of fear
423 responses in zebrafish. *Nat. Neurosci.* 13, 1354–1356. doi:10.1038/nn.2654.
- 424 Agranoff, B. W., and Davis, R. E. (1968). “The use of fishes in studies on memory
425 formation,” in *The Central Nervous System and Fish Behavior* (University of
426 Chicago Press Chicago).
- 427 Aizenberg, M., and Schuman, E. M. (2011). Cerebellar-Dependent Learning in Larval
428 Zebrafish. *J. Neurosci.* 31, 8708–8712. doi:10.1523/JNEUROSCI.6565-10.2011.
- 429 Arthur, D., and Levin, E. (2001). Spatial and non-spatial visual discrimination
430 learning in zebrafish (*Danio rerio*). *Anim. Cogn.* doi:10.1007/s100710100111.
- 431 Bradski, G. (2000). The OpenCV Library. *Dr Dobbs J. Softw. Tools.*
432 doi:10.1111/0023-8333.50.s1.10.
- 433 Buske, C., and Gerlai, R. (2014). Diving deeper into Zebrafish development of social
434 behavior: Analyzing high resolution data. *J. Neurosci. Methods.*
435 doi:10.1016/j.jneumeth.2014.06.019.

- 436 Chen, X., and Engert, F. (2014). Navigational strategies underlying phototaxis in
437 larval zebrafish. *Front. Syst. Neurosci.* doi:10.3389/fnsys.2014.00039.
- 438 Cong, L., Wang, Z., Chai, Y., Hang, W., Shang, C., Yang, W., et al. (2017). Rapid
439 whole brain imaging of neural activity in freely behaving larval zebrafish (*Danio*
440 *rerio*). *Elife*. doi:10.7554/eLife.28158.
- 441 Cunliffe, V. T. (2003). Zebrafish: A Practical Approach. *Genet. Res.* 82,
442 S0016672303216384. doi:10.1017/S0016672303216384.
- 443 Davis, R. E., and Agranoff, B. W. (1966). Stages of memory formation in goldfish:
444 evidence for an environmental trigger. *Proc. Natl. Acad. Sci. U. S. A.* 55, 555–9.
445 doi:10.1073/PNAS.55.3.555.
- 446 Freund, G., and Walker, D. W. (1972). Operant conditioning in mice. *Life Sci.*
447 doi:10.1016/0024-3205(72)90042-2.
- 448 Gehrig, J., Pandey, G., and Westhoff, J. H. (2018). Zebrafish as a Model for Drug
449 Screening in Genetic Kidney Diseases. *Front. Pediatr.* 6, 183.
450 doi:10.3389/fped.2018.00183.
- 451 Guggiana-Nilo, D. A., and Engert, F. (2016). Properties of the Visible Light
452 Phototaxis and UV Avoidance Behaviors in the Larval Zebrafish. *Front. Behav.*
453 *Neurosci.* doi:10.3389/fnbeh.2016.00160.
- 454 Hinz, F. I., Aizenberg, M., Tushev, G., and Schuman, E. M. (2013). Protein
455 Synthesis-Dependent Associative Long-Term Memory in Larval Zebrafish. *J.*
456 *Neurosci.* 33, 15382–15387. doi:10.1523/JNEUROSCI.0560-13.2013.
- 457 Ingebretson, J. J., and Masino, M. A. (2013). Quantification of locomotor activity in
458 larval zebrafish: considerations for the design of high-throughput behavioral
459 studies. *Front. Neural Circuits.* doi:10.3389/fncir.2013.00109.
- 460 Ishikawa, D., Matsumoto, N., Sakaguchi, T., Matsuki, N., and Ikegaya, Y. (2014).
461 Operant conditioning of synaptic and spiking activity patterns in single
462 hippocampal neurons. *J. Neurosci.* doi:10.1523/JNEUROSCI.5298-13.2014.
- 463 Kim, D. H., Kim, J., Marques, J. C., Grama, A., Hildebrand, D. G. C., Gu, W., et al.
464 (2017). Pan-neuronal calcium imaging with cellular resolution in freely
465 swimming zebrafish. *Nat. Methods* 14, 1107–1114. doi:10.1038/nmeth.4429.
- 466 Kokel, D., Bryan, J., Laggner, C., White, R., Cheung, C. Y. J., Mateus, R., et al.
467 (2010). Rapid behavior-based identification of neuroactive small molecules in
468 the zebrafish. *Nat. Chem. Biol.* 6, 231–237. doi:10.1038/nchembio.307.
- 469 Leifer, A. M., Fang-Yen, C., Gershow, M., Alkema, M. J., and Samuel, A. D. T. (2011).
470 Optogenetic manipulation of neural activity in freely moving *Caenorhabditis*
471 *elegans*. *Nat. Methods* 8, 147–152. doi:10.1038/nmeth.1554.
- 472 Li, J. M. (2012). Identification of an Operant Learning Circuit by Whole Brain
473 Functional Imaging in Larval Zebrafish. Doctoral dissertation, Harvard

- 474 University. Available at: <http://nrs.harvard.edu/urn-3:HUL.InstRepos:10974703>.
- 475 Mirat, O., Sternberg, J. R., Severi, K. E., and Wyart, C. (2013). ZebraZoom: an
476 automated program for high-throughput behavioral analysis and categorization.
477 *Front. Neural Circuits*. doi:10.3389/fncir.2013.00107.
- 478 Mueller, T., and Wullimann, M. F. *Atlas of early zebrafish brain development : a tool*
479 *for molecular neurogenetics*. 2nd Edition.
- 480 Myers, K. M., and Davis, M. (2007). Mechanisms of fear extinction. *Mol. Psychiatry*.
481 doi:10.1038/sj.mp.4001939.
- 482 Pelkowski, S. D., Kapoor, M., Richendrfer, H. A., Wang, X., Colwill, R. M., and
483 Creton, R. (2011). A novel high-throughput imaging system for automated
484 analyses of avoidance behavior in zebrafish larvae. *Behav. Brain Res.* 223, 135–
485 144. doi:10.1016/J.BBR.2011.04.033.
- 486 Rihel, J., Prober, D. A., Arvanites, A., Lam, K., Zimmerman, S., Jang, S., et al. (2010).
487 Zebrafish behavioral profiling links drugs to biological targets and rest/wake
488 regulation. *Science* 327, 348–51. doi:10.1126/science.1183090.
- 489 Skinner, B. F. (1984). The evolution of behavior. *J. Exp. Anal. Behav.* 41, 217–221.
490 doi:10.1901/jeab.1984.41-217.
- 491 Steenbergen, P. J., Richardson, M. K., and Champagne, D. L. (2011). Patterns of
492 avoidance behaviours in the light/dark preference test in young juvenile zebrafish:
493 A pharmacological study. *Behav. Brain Res.* 222, 15–25.
494 doi:10.1016/j.bbr.2011.03.025.
- 495 Valente, A., Huang, K. H., Portugues, R., and Engert, F. (2012). Ontogeny of classical
496 and operant learning behaviors in zebrafish. *Learn. Mem.* 19, 170–177.
497 doi:10.1101/lm.025668.112.
- 498 Yang, X., Jounaidi, Y., Dai, J. B., Marte-Oquendo, F., Halpin, E. S., Brown, L. E., et
499 al. (2018). High-throughput Screening in Larval Zebrafish Identifies Novel
500 Potent Sedative-hypnotics. *Anesthesiology*.
501 doi:10.1097/ALN.0000000000002281.
- 502 Zhang, B. bing, Yao, Y. yuan, Zhang, H. fei, Kawakami, K., and Du, J. lin (2017). Left
503 Habenula Mediates Light-Preference Behavior in Zebrafish via an Asymmetrical
504 Visual Pathway. *Neuron* 93, 914–928.e4. doi:10.1016/j.neuron.2017.01.011.
- 505
- 506
- 507
- 508
- 509

510 **Table 1. Visual intensity ratios of all visual patterns to the pure-gray pattern**

	White-black checkerboard	Red-black checkerboard	Pure black pattern	Pure gray pattern
Mean RGB value	(128,128,128)	(128,0,0)	(0,0,0)	(128,128,128)
Grayscale value	128	43	0	128
Intensity ratio to the pure-gray pattern	1	0.34	0.0	1

511 In the table, each column stands for a visual pattern used in the experiment and rows
 512 show the mean values, the grayscale values, and the contrast ratios to the pure-gray
 513 pattern (the pattern at the non-CS zone, see Methods).

514

515 **Table 2. Comparison of learning response increment between different**
 516 **conditioned patterns**

	White-black Checkerboard	Red-black Checkerboard	Pure Black Pattern
Positional Index Increment	0.0015 (p = 0.8832)	0.0386 (p = 0.0021)	0.1010 (p = 5.92 x 10 ⁻⁶)
Turning Index Increment	-0.0239 (p = 0.3705)	0.0599 (p = 0.0099)	0.1103 (p = 0.0057)

517 In the table, each column stands for each conditioned visual stimulus used in the
 518 experiment and rows show the positional index increment and the turning index
 519 increment. (t-test)

520

521 **Table 3. Age-dependent learning ratio and memory length (CS zone was**
 522 **red-black checkerboard)**

	7	8	9	10	Total
Learning Ratio	4/16	4/19	6/29	13/40	27/104
Memory Length (s)	450	690	740	877	756

523 In the table, each column stands for fish age and rows show the learning ratio and
 524 memory length.

525

526 **Table 4. Age-dependent learning ratio and memory length (CS zone was**
527 **pure-black pattern)**

	7	8	9	10	Total
Learning Ratio	4/10	7/10	6/12	4/10	21/42
Memory Length (s)	840	1080	940	960	971

528 In the table, each column stands for fish age and rows show the learning ratio and
529 memory length.

530

531

532 **Figure 1. Larval zebrafish show significant learning responses in the operant**
533 **learning task.**

534 (A) Schematics of the behavioral system. Each arena holds one fish. Cameras,
535 projector, relay are controlled by the custom software BLITZ. Software ABLITZER
536 imports the BLITZ-produced behavioral data, analyzes them and visualizes the results.

537 (B) Operant learning paradigm. The procedure (top) and the detailed protocol in the
538 training stage (bottom).

539 (C) Larval zebrafish showed significant learning responses, quantified by the
540 positional index, after operational conditioning. Each bar pair shows the positional
541 indices before (light bar) and after (black bar) the training ($p = 0.0843$, $p = 0.0021$, and
542 $p = 0.1260$ from left to right, t-test).

543 (D) Larval zebrafish showed significant learning responses, quantified by the turning
544 index, after operational conditioning ($p = 0.1836$, $p = 0.0099$, and $p = 0.0628$, t-test).

545 (E) A representative behavioral trace. A typical learner's relative position to the
546 midline during an operant learning experiment (CS zone: red-black checkerboard,
547 non-CS zone: pure gray pattern). A positive distance suggests fish in the non-CS zone
548 (also see Methods). Each red dot represents the delivery of one electroshock.

549

550 **Figure 2. Visual intensity ratios modulate operant learning responses in larval**
551 **zebrafish.**

552 (A) Analysis of the positional index suggested that fish did not show significant
553 learning responses (CS zone was white-black checkerboard). t-test, $p = 0.8832$ for the
554 experiment group, $p = 0.2493$ for the self-control group. There is no unpaired-control
555 group because no significant learning responses were found in the experiment group.

556 (B) Analysis of the turning index suggested that fish did not show significant learning
557 responses (CS zone was white-black checkerboard). t-test, $p = 0.3750$ for the
558 experiment group, $p = 0.7089$ for the self-control group. There is no unpaired-control
559 group because no significant learning responses were found in the experiment group.

560 (C) Analysis of the positional index suggested that fish showed significant learning
561 responses. (CS zone was black pattern; $p = 0.2018$, $p < 0.0001$, $p = 0.1923$, from left to
562 right respectively, t-test.)

563 (D) Analysis of the turning index suggested that fish showed significant learning
564 responses. (CS zone was black pattern; $p = 0.2811$, $p = 0.0057$, and $p = 0.9837$, from
565 left to right respectively, t-test.)

566

567 **Figure 3. Single fish analysis distinguishes learners from non-learners.**

568 (A) Positional index averaged over all fish in the experiment group as well as the
569 subpopulations classified as learners (light solid line, $N = 21$) and non-learners (light
570 dash line, $N = 21$). CS zone was black pattern and the entire training process was
571 divided into two-minute-epochs.

572 (B) Analysis of the positional index suggested that the learners ($N = 21$) showed
573 significant learning responses before and after training; whereas the non-learners ($N =$
574 21) did not show significant learning responses. (CS zone was black pattern; t-test, $p =$
575 $1.98e-11$ for the learners, $p = 0.9492$ for the non-learners and $p = 2.03e-06$ for all fish.)

576 (C) Learners also showed significant difference in the turning indices. (CS zone was
577 black pattern; t-test, $p = 1.22e-5$ for the learners, $p = 0.6491$ for the non-learners and $p =$
578 0.0057 for all fish.)

579 (D) Positional index averaged over all fish in the experiment group as well as the
580 subpopulations classified as learners (light solid line, $N = 27$) and non-learners (light
581 dash line, $N = 77$). CS zone was red-black checkerboard; same analysis as in (A).

582 (E) Learners showed significant difference in the positional indices, the same analysis
583 as in (B). (CS zone was red-black checkerboard; t-test, $p = 6.52e-12$ for the learners, $p =$
584 0.3849 for the non-learners and $p = 0.0020$ for all fish.)

585 (F) Learners also showed significant difference in the turning indices, same analysis
586 as in (C). (CS zone was red-black checkerboard; t-test, $p = 2.28e-6$ for the learners, $p =$
587 0.8606 for the non-learners and $p = 0.0099$ for all fish.)

588 (G) A typical trace of a learner whose memory would extinct during the test phase (CS
589 zone was red-black checkerboard). The blue triangle denotes the extinction point when
590 the single-epoch-averaged positional index drops below the mean index of the baseline.

591 (H) A magnification of the test phase in (G).

592 (I) Distributions of memory lengths of learners when CS zone was red-black
593 checkerboard or pure black pattern respectively.

594

595 **Figure 4. Age-dependent operant learning ability in larval zebrafish**

596 (A) The mean memory length of all learners at specific age (CS zone was red-black
597 checkerboard). Error bars are S.E.M. Linear regression was applied (red dashed line) to
598 show the statistical trend. (Bi-square fitting applied, $R\text{-square} = 0.932$, $p = 0.0347$)

599 (B) The mean positional index increment (CS zone was red-black checkerboard), the
600 same analysis as in (A). (Bi-square fitting applied, $R\text{-square} = 0.915$, $p = 0.0434$)

601 (C) The mean turning index increment (CS zone was red-black checkerboard), the
602 same analysis as in (A). (Bi-square fitting applied, $R\text{-square} = 0.237$, $p = 0.5130$)

603 (D) The mean memory length of all learners at specific ages (CS zone was pure-black
604 pattern), same analysis as in (A). (Bi-square fitting applied, $R\text{-square} = 0.033$, $p =$
605 0.8190)

- 606 (E) The mean positional index increment (CS zone was pure-black pattern), the same
607 analysis as in (A). (Bi-square fitting applied, R-square = 0.229, p = 0.5210)
- 608 (F) The mean turning index increment (CS zone was pure-black pattern); the same
609 analysis as in (A). (Bi-square fitting applied, R-square = 0.688, p = 0.1710)

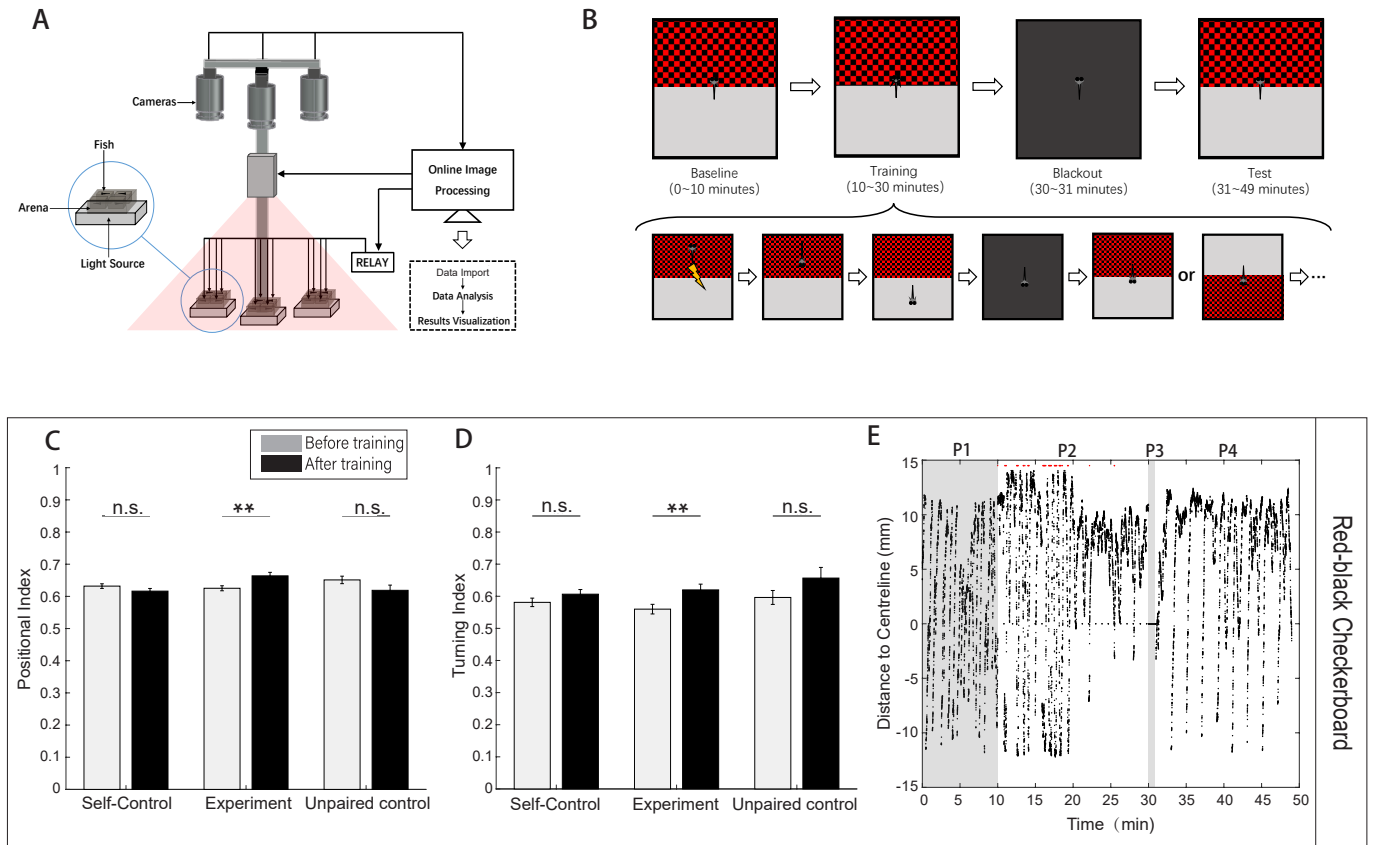


Figure 1. Larval zebrafish show significant learning responses in the operant learning task.

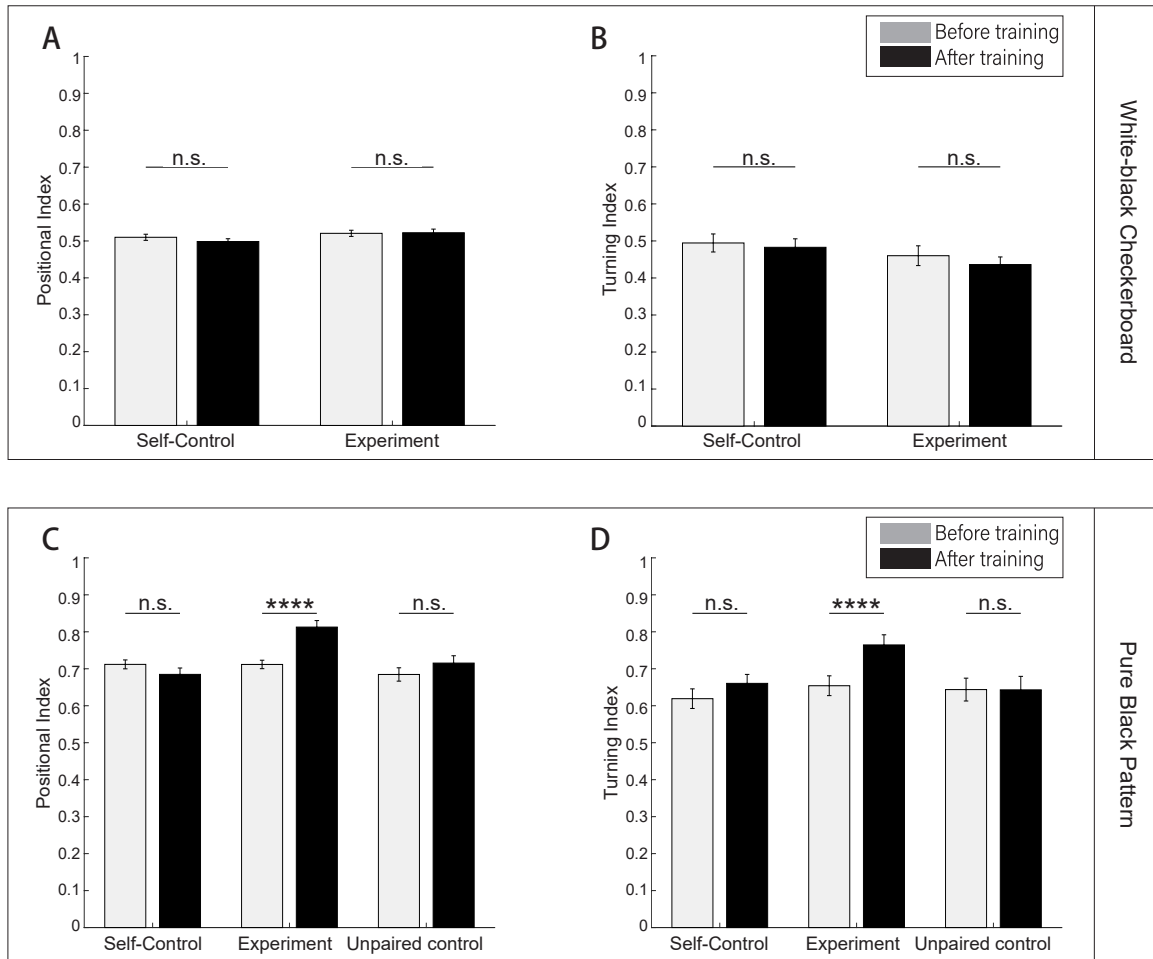


Figure 2. Visual intensity ratios modulate operant learning responses in larval zebrafish.

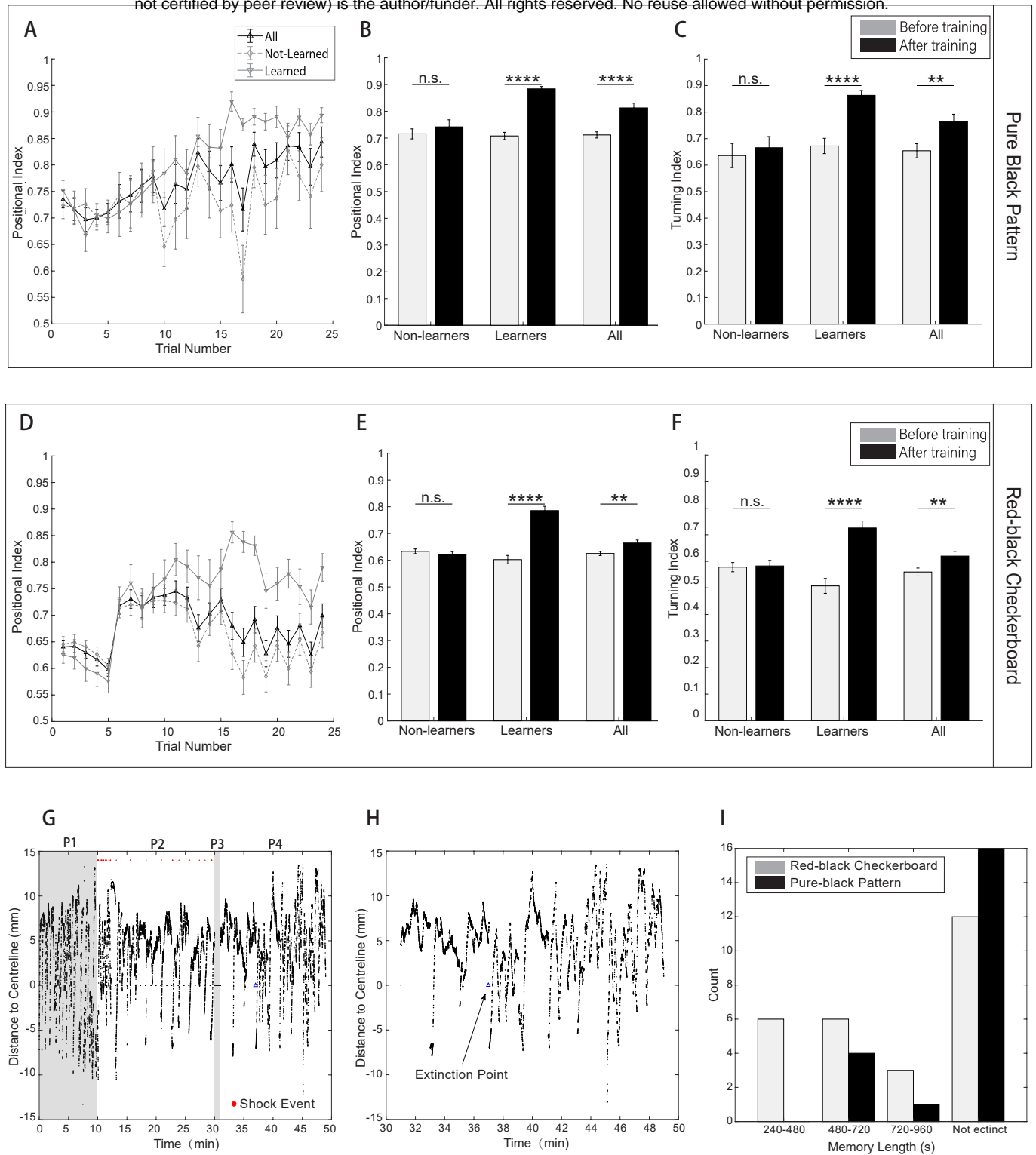


Figure 3. Single fish analysis distinguishes learners from non-learners.

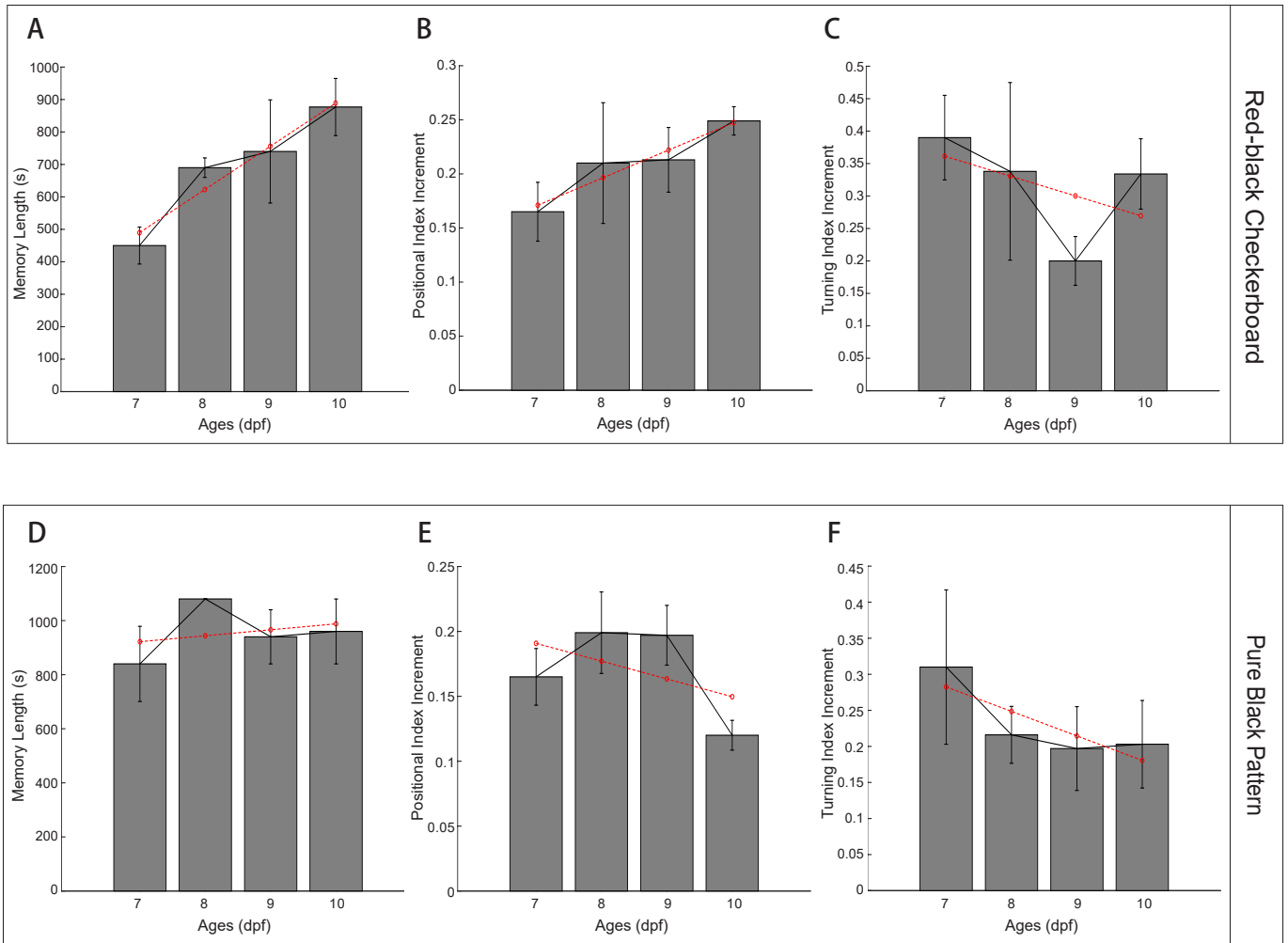


Figure 4. Age-dependent operant learning ability in larval zebrafish